Supporting Information

Biodegradable Nitrogen-Doped Carbon Nanodots for Non-Invasive Photoacoustic Imaging and Photothermal Therapy

Changho Lee[1§¶], Woosung Kwon[2§], Songeun Beack[3§], Donghyun Lee[1], Yoonsang Park[4], Heymin Kim[3], Sei Kwang Hahn[3], Shi-Woo Rhee,[2,4]*, & Chulhong Kim[1]**

[1]Department of Creative IT Engineering, Pohang University of Science and Technology (POSTECH), 77 Cheongam-ro, Pohang 37673, South Korea

[2]Department of Chemical and Biological Engineering, Sookmyung Women's University, 100 Cheongpa-ro 47-gil, Seoul 04310, South Korea

[3]Department of Materials and Science Engineering, Pohang University of Science and Technology (POSTECH), 77 Cheongam-ro, Pohang 37673, South Korea

[4]Department of Chemical Engineering, Pohang University of Science and Technology (POSTECH), 77 Cheongam-ro, Pohang 37673, South Korea

*[§]These authors contributed equally to this work. *Correspondence and requests for materials should be addressed to S.K.H. (email: skhanb@postech.edu), S.-W.R. (email:srhee@sookmyung.ac.kr), & C.K. (email:chulhong@postech.edu).*

[¶]Current address: Department of Electrical and Computer Engineering, Johns Hopkins University, 3400 North Charles Street, Baltimore, MD 21218, USA

Quantum yield (QY) measurement of N-CNDs. The QY measurement of N-CNDs (in water) were performed using IR-26 in 1,2-dichloroethane as a reference (QY = 0.5%). A series of IR-26 and N-CND solutions that exhibited absorbance values of 0.02, 0.04, 0.06, 0.08, and 0.1 at 808 nm were prepared by adjusting the solution concentrations. Absorbance spectra of IR-26 and N-CNDs were recorded on a Scinco S-3100 spectrophotometer. Fluorescence spectra of IR-26 and N-CNDs were recorded on a Horiba Nanolog fluorometer. 1-cm-path QS-grade quartz cuvettes (Hellma Analytics 111-QS) were used for all optical experiments. The QY of N-CNDs was calculated according to the following equation:

$$\mathrm{QY} = \mathrm{QY}_{\mathrm{IR-26}} \frac{\mathrm{S}}{\mathrm{S}_{\mathrm{IR-26}}} \left(\frac{n}{n_{\mathrm{IR-26}}} \right)$$

where S is the slope of the fitted line and *n* is the refractive index.

Preparation of GNR. GNR was synthesized as reported elsewhere [1]. In brief, a seed solution was made by mixing 0.2 M of CTAB and 5 mL of $HAuCl_4$ solution. Next, 600 µL of freshly prepared 10-mM ice-cold $NaBH_4$ solution was poured into the reaction solution. The mixture was stirred for 2 h. A growth solution was prepared by mixing 50 mL of CTAB and 50 mL of 1 mM $HAuCl_4$ with 150 µL of 10-mM silver nitrate aqueous solution. After mixing the solution, 550 µL of 0.1 M ascorbic acid was added. While continuously stirring this mixture, 100 µL of the seed solution was added to the growth solution. These nanorods were stirred for 24 h to stabilize the full growth. After termination of the reaction, excess CTAB was removed by centrifuging at 12,000 rpm, and the pellets were dispersed in the DI water. The morphology and size of the as-synthesized GNRs were characterized by TEM (JEM 1011 operated at 80 kV). The length and diameter of GNRs are 36.41 ± 2.23 nm and 2.20 ± 0.23 nm, respectively. To quantify the mass of gold in the GNRs, an inductively coupled plasma mass spectrometry (ICP-MS) experiment was performed.

The photothermal conversion efficiency. The photothermal conversion efficiency of N-CNDs was calculated by following equation (1) [2, 3].

$$\eta = \frac{hS(T_{max} - T_{surr}) - Q_{diss}}{I(1 - 10^{-Abs_{808}})} \quad (1)$$

h indicates the heat transfer coefficient. S indicates the surface area of the sample container. T_{max} and T_{surr} indicate the maximum steady temperature (i.e., 52.5 ℃) and the environmental tempearaure (i.e., 25.0 ℃) of the solution N-CNDs, respectively. I indicates the used laser power, which is 2000 mW. Abs_{808} is the absorbance of N-CNDs at 808 nm, measured as 0.109. Q_{diss} is heat dissipated from the light absorbed by the sample container, which is 0.23 mW. Frist, hS can be calculated by equation (2).

$$hS = \frac{mc}{\tau_s} \quad (2)$$

To caluclate hS, a dimesionelss parameter θ should be acuqired by following equation (3).

$$\theta = \frac{T - T_{Surr}}{T_{MAX} - T_{Surr}} \quad (3)$$

Then, the constant for sample system time τ_s can be estimated by following eaquation (4).

$$t = -\tau_s ln(\theta) \quad (4)$$

The calculated $\tau_s$values from eaqaution (3) and (4) is 136.16 s. m and c are 0.02 g and 4.2 J/g·℃, respectivley. Finally, the calculated photothermal conversion efficiency at 808 nm (η) is about 3.77%.

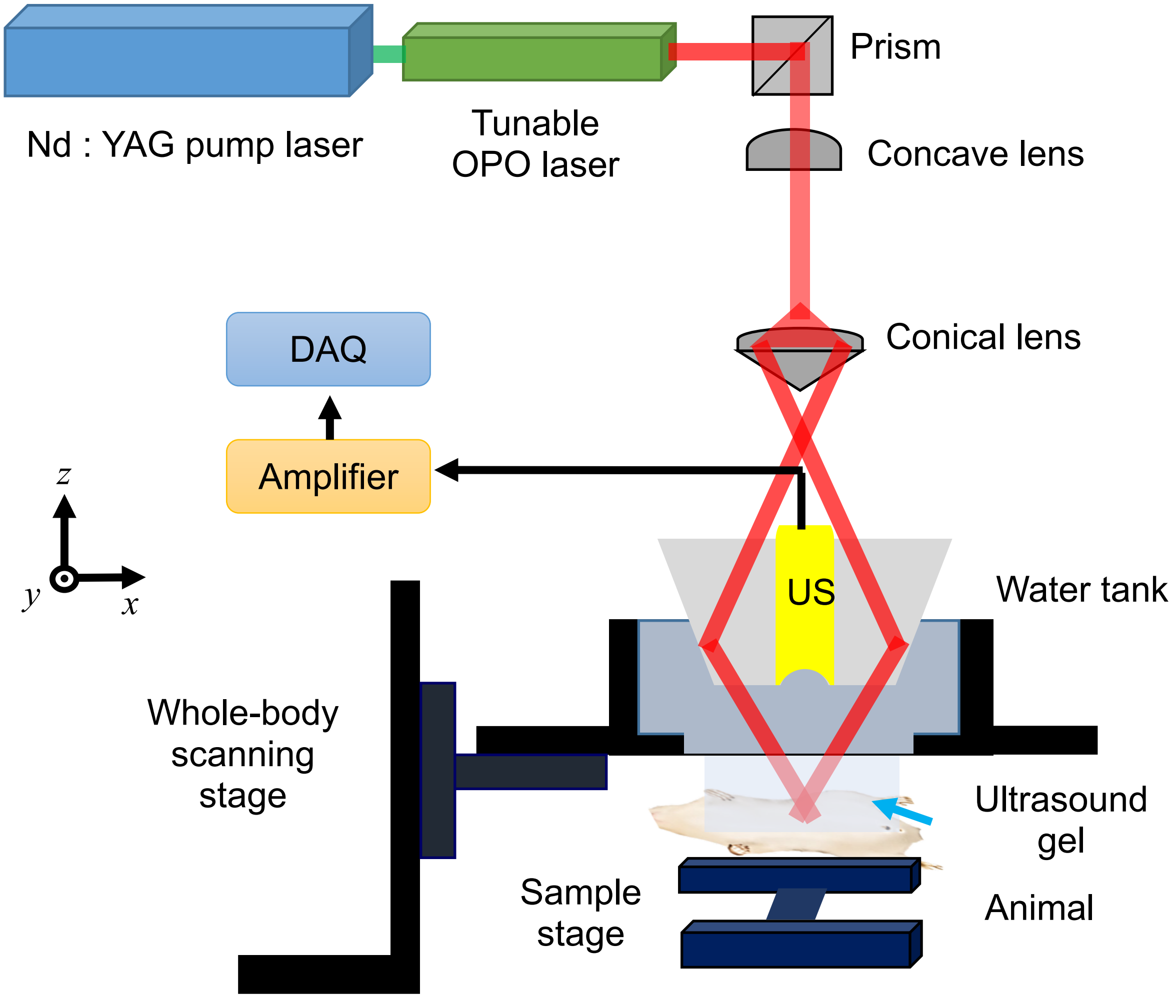

Figure S1. Schematic of the acoustic-resolution reflection-mode PA imaging system.

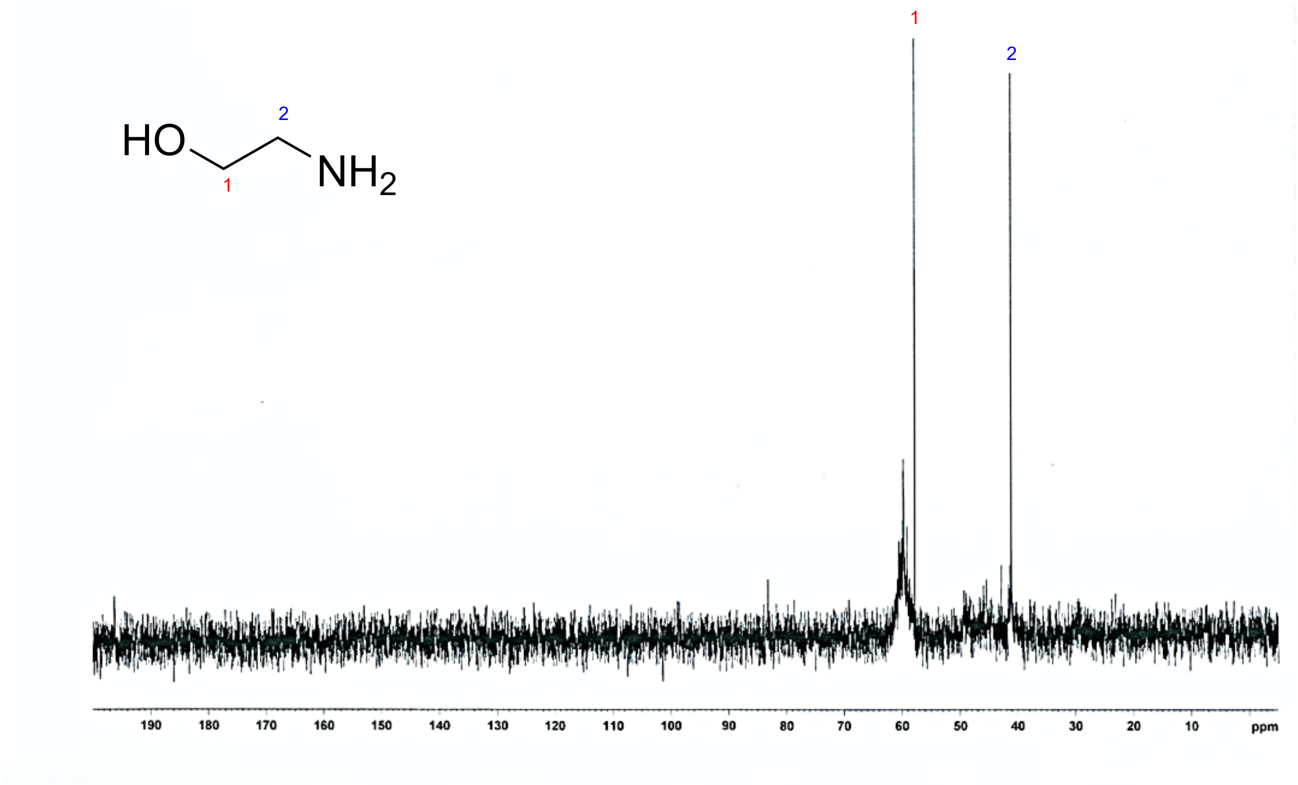

Figure S2. ^{13}C-NMR analysis of ethanolamine-functionalized CNDs.

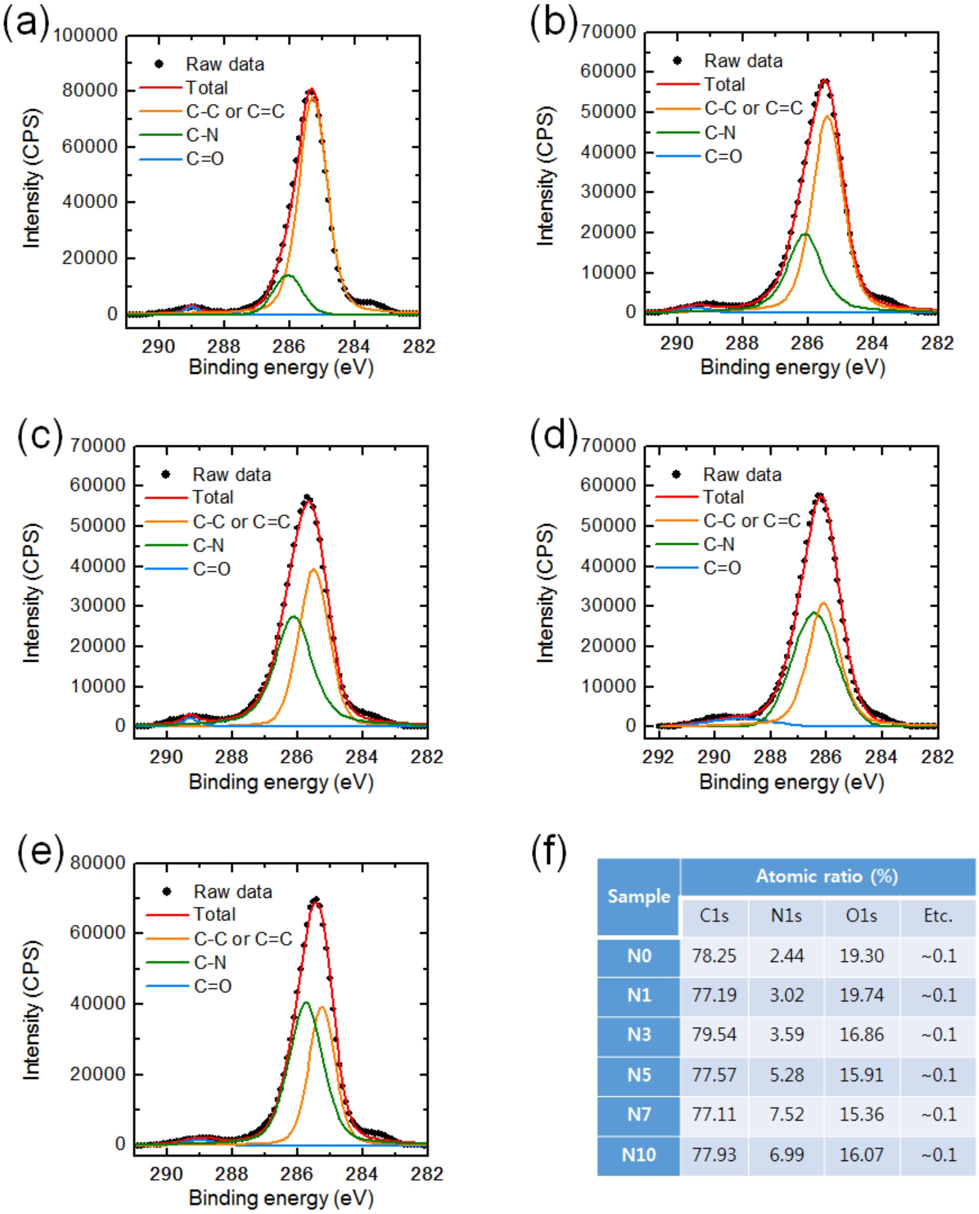

Sample	Atomic ratio (%)			
	C1s	N1s	O1s	Etc.
N0	78.25	2.44	19.30	~0.1
N1	77.19	3.02	19.74	~0.1
N3	79.54	3.59	16.86	~0.1
N5	77.57	5.28	15.91	~0.1
N7	77.11	7.52	15.36	~0.1
N10	77.93	6.99	16.07	~0.1

Figure S3. X-ray photoelectron spectra (C1s) of (a) N0-, (b) N1-, (c) N3-, (d) N5-, (e) N7-CNDs, and the atomic contents of the N-CNDs. The C1s XPS data show peaks centered from 285.3–286.2 eV, and each of these peaks can be deconvoluted into three major contributions: C - C/C = C (285.2–286.1 eV), C -N (286.1–286.5 eV), and C = O (289.3 eV). The intensity ratio of C - N to C - C/C = C gradually increased with increasing nitric acid molarities, which indicated that the nitrogen content of the CNDs was proportional to the nitric acid molarities.

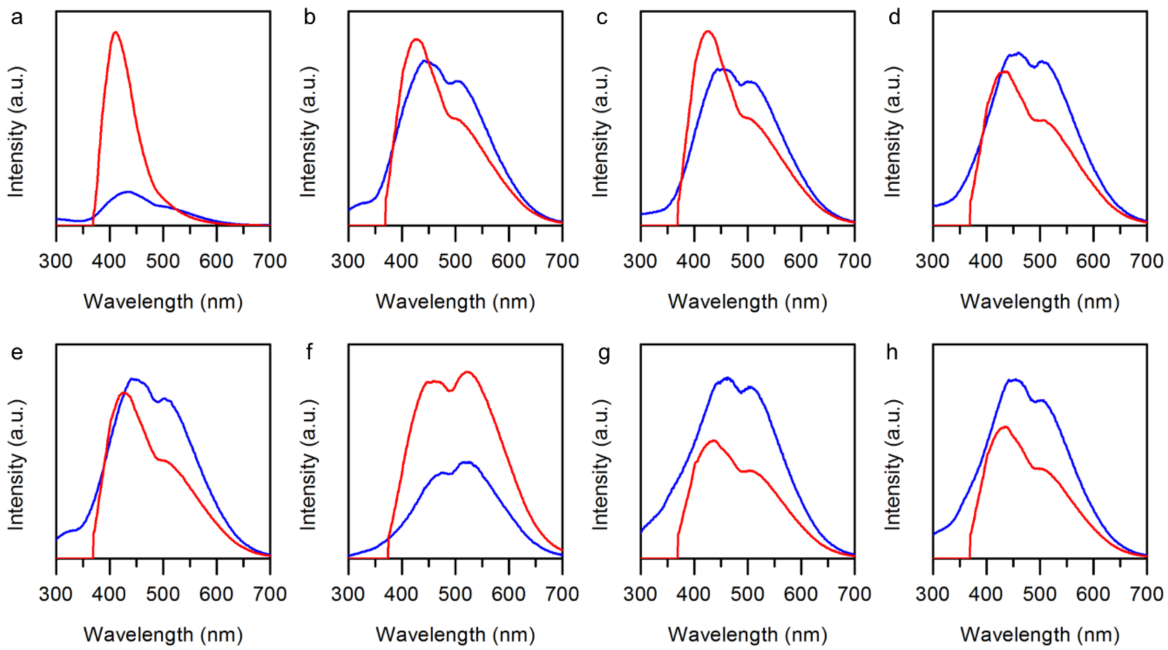

Figure S4. Photoluminescence spectra of (a) N0-, (b) N1-, (c) N3-, (d) N5-, (e) N7-, (f) N10-, (g) N12-, and (h) N14-CNDs at 270 nm (blue) and 360 nm (red) excitation wavelengths. As the nitrogen content is increased, a secondary peak is developed at around 500 nm, which can be assigned to enhanced n→π* transition due to additional non-bonding orbitals (or lone pairs of electrons) generated by the incorporated nitrogen atoms.

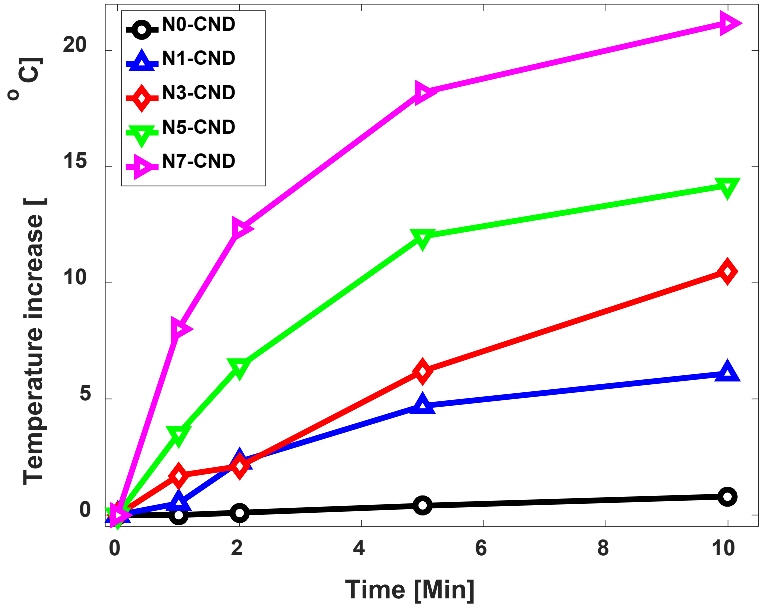

Figure S5. Temperature increase of different N-doped CNDs with near-infrared (wavelength = 680–808 nm) laser excitation.

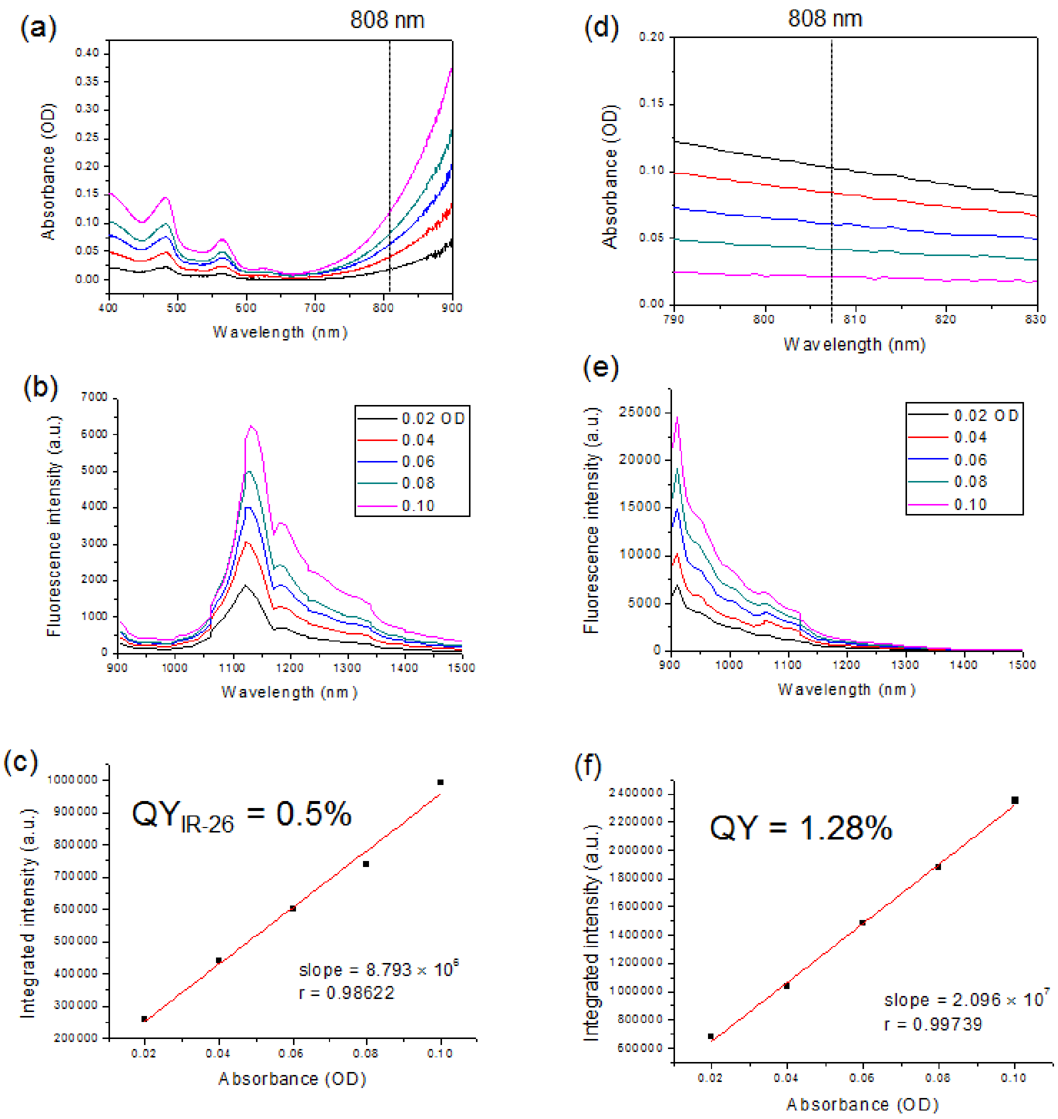

Figure S6. Quantum yield (QY) measurement of N-CNDs using IR-26 in 1,2-dichloroethane as a reference (QY = 0.5 %). (a) Absorption spectra of a series of solutions of IR-26 in 1,2-dichloroethane that exhibited absorbance values of ~0.02, ~0.04, ~0.06, ~0.08, and ~0.10 at 808 nm. (b) Fluorescence spectra of the IR-26 solutions under 808-nm excitation. (c) The integrated intensities of the IR-26 solutions plotted versus the absorbance values at 808 nm. The slope was calculated by linear fitting. (d) Absorption spectra of a series of solutions of N-CNDs in water that exhibit absorbance values of ~0.02, ~0.04, ~0.06, ~0.08, and ~0.10 at 808 nm. (e) Fluorescence spectra of N-CND solutions under 808-nm excitation. (f) The integrated intensities of the N-CND solutions plotted versus the absorbance values at 808 nm. The slope was calculated by linear fitting. The QY of N-CNDs was found to be 1.28%.

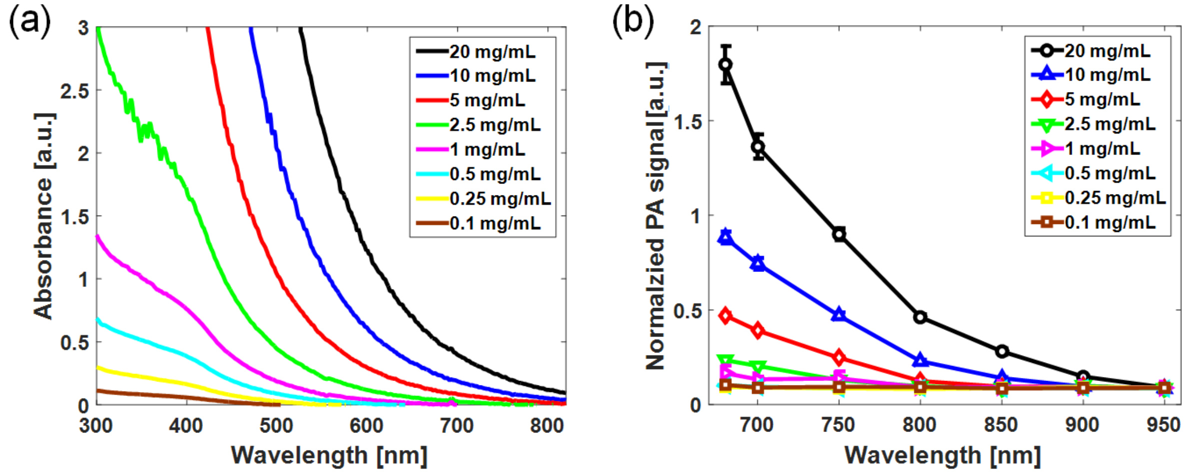

Figure S7. (a) Optical absorption of N-CNDs, (b) Photoacoustic spectrum of N-CNDs at a different concentration.

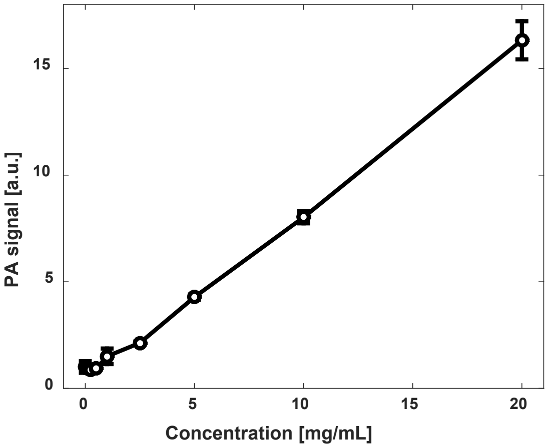

Figure S8. PA signal sensitivity at 680 nm with increasing concentration of N-CNDs.

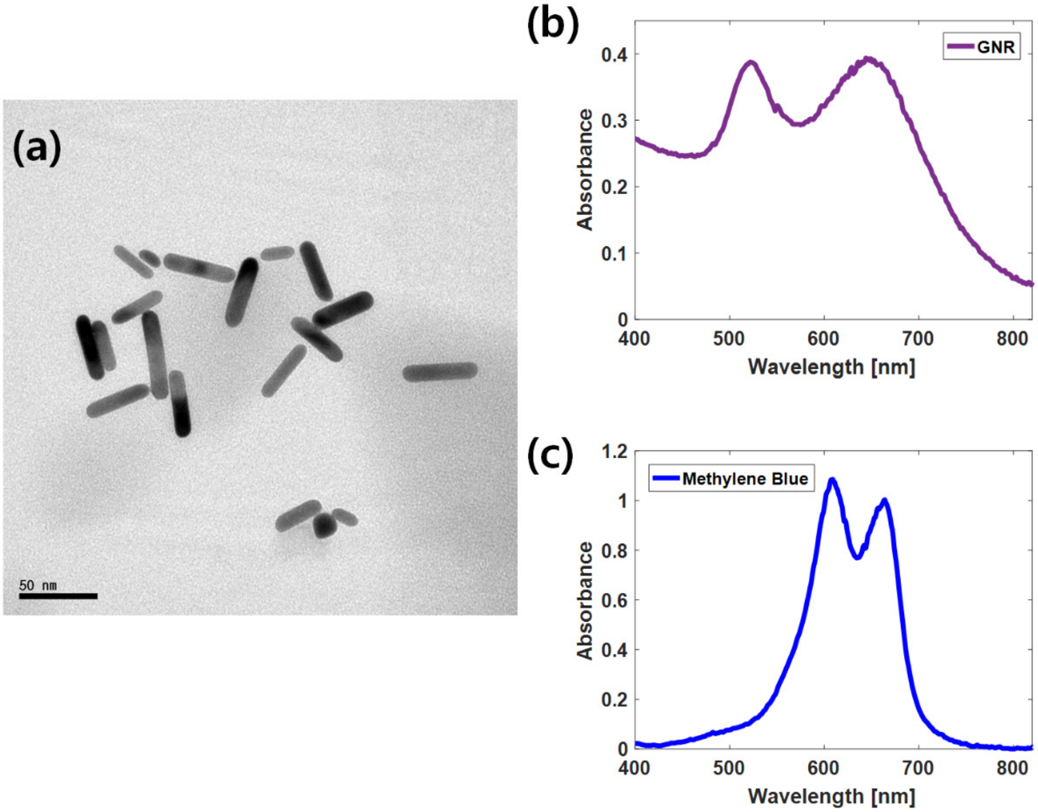

Figure S9. (a) TEM image of GNR, (b) UV spectrum of GNR, and (c) UV-spectrum of methylene blue.

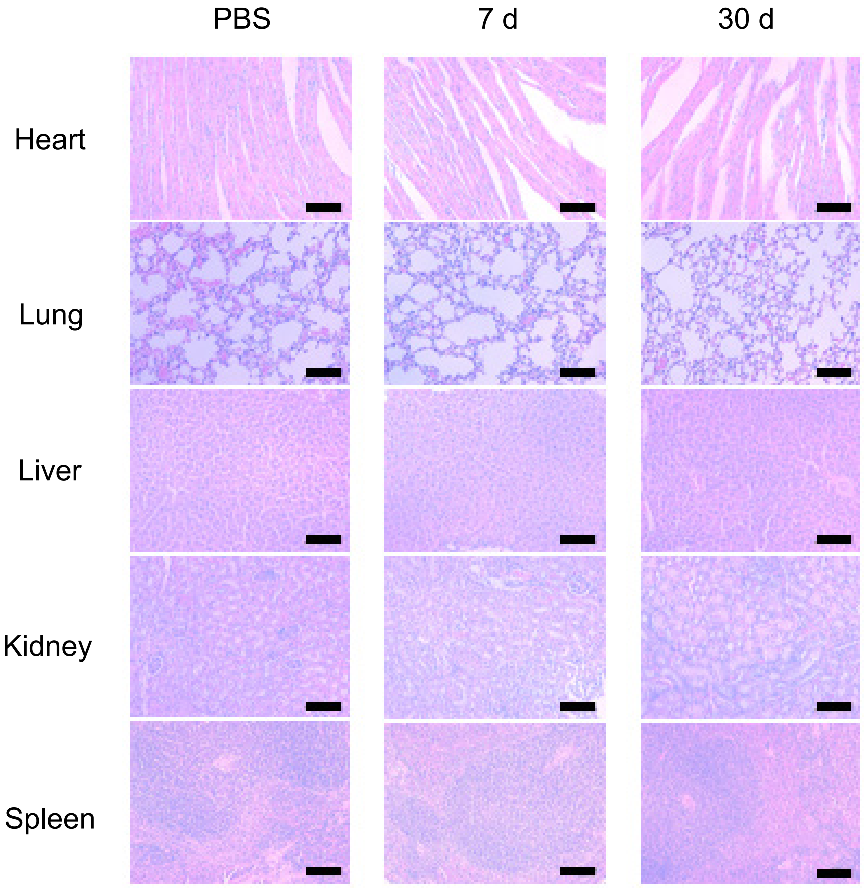

Figure S10. *In vivo* safety of N-CNDs assessed using histological analysis (scale bar = 100 μm).

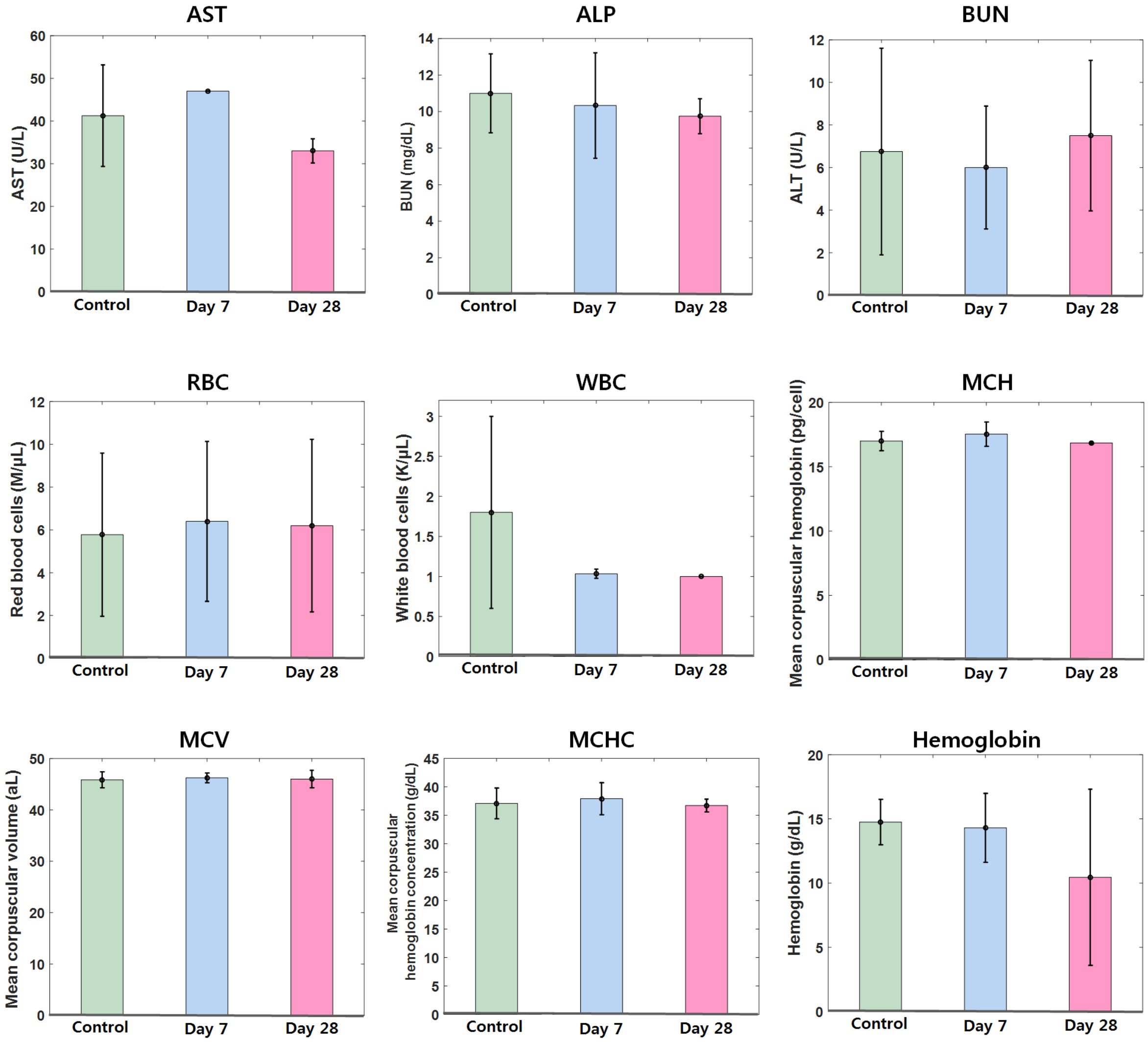

Figure S11. *In vivo* cytocompatibility of N-CNDs. Blood biochemistry assay of mice 1 month after intravenous injection of PBS as a control and N-CNDs after 7 days and 28 days.

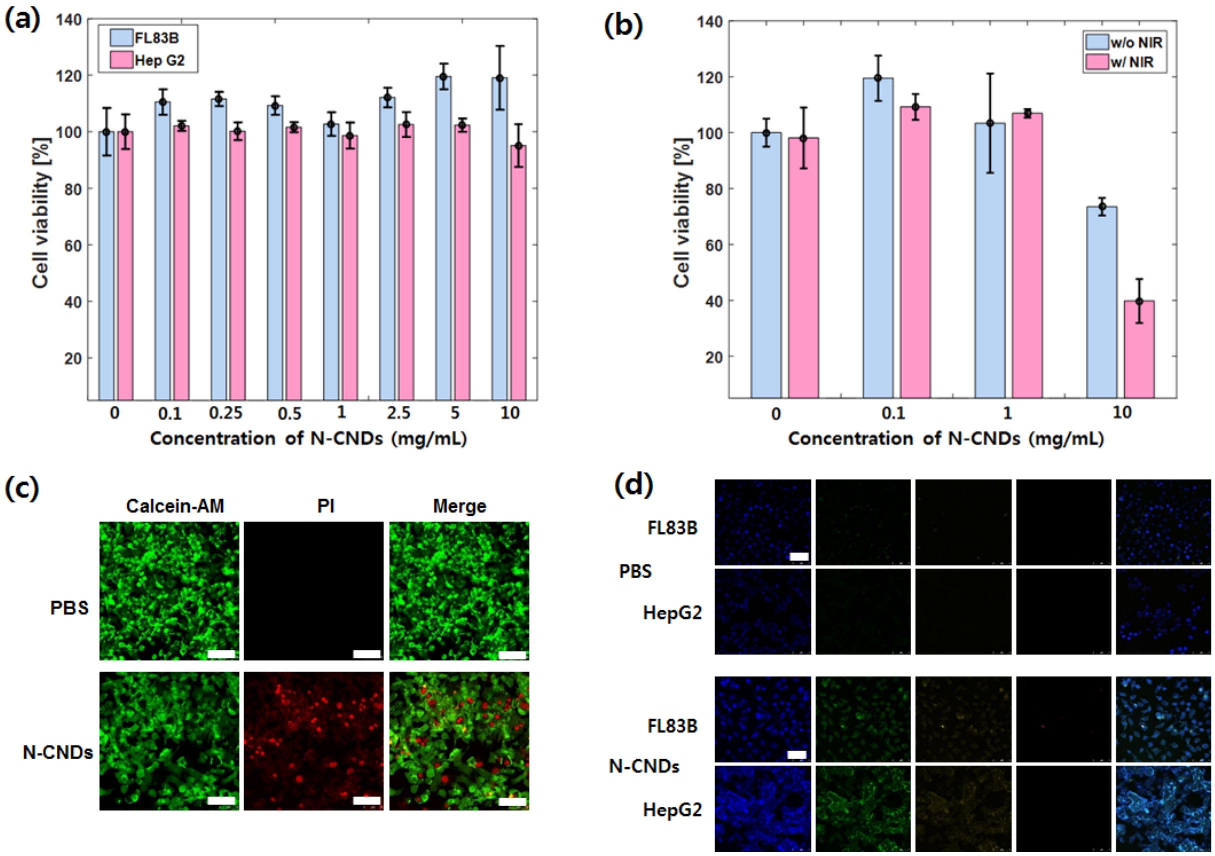

Figure S12. *In vitro* test of N-CNDs. (a) Cytotoxicity of N-CNDs in normal liver cells and liver cancer cells without NIR laser irradiation. (b) *In vitro* PTT test of N-CNDs without and with NIR laser irradiation. (c) Live/dead assay after *in vitro* PTT with N-CNDs. (d) Confocal images for detection of cellular uptake of N-CNDs. (Scale bar = 100 μm)

References

1. Nikoobakht B, El-Sayed MA. Preparation and growth mechanism of gold nanorods (NRs) using seed-mediated growth method. Chemistry of Materials. 2003; 15: 1957-62.
2. Hessel CM, Pattani VP, Rasch M, Panthani MG, Koo B, Tunnell JW, et al. Copper selenide nanocrystals for photothermal therapy. Nano letters. 2011; 11: 2560-6.
3. Tian Q, Jiang F, Zou R, Liu Q, Chen Z, Zhu M, et al. Hydrophilic Cu9S5 nanocrystals: A photothermal agent with a 25.7% heat conversion efficiency for photothermal ablation of cancer cells in vivo. ACS nano. 2011; 5: 9761-71.